Geophys. J. R. astr. Soc. (1978) **54**, 43–60

LISPB – IV. Crustal structure of Northern Britain

D. Bamford* *Department of Geophysics, University of Edinburgh*
K. Nunn *Department of Geological Sciences, University of Birmingham*
C. Prodehl *Geophysikalisches Institut, Universität, Karlsruhe, Germany*
B. Jacob† *IGS Seismology Unit, Edinburgh*

Received 1977 September 28

Summary. This paper presents those results from the 1974 Lithospheric Seismic Profile in Britain (LISPB) which relate to the compressional velocity structure of the crust and uppermost mantle beneath Northern Britain. A combination of interpretation techniques suitable for modelling laterally inhomogeneous media, including two-dimensional ray-tracing and time-term analysis, has resulted in a detailed seismic cross-section across the Caledonian orogenic belt. The main features of this section are a possible horizontal discontinuity in the Pre-Caledonian basement, a change in the relationship between the lower crust and the uppermost mantle from north to south and a considerable thickening of the crust beneath the Caledonian fold belt. These results place considerable constraints upon tectonic models for the evolution of the Caledonides in particular in their implication of differing crustal structures north and south of the Southern Uplands and their indication of the primary significance of the Southern Uplands Fault.

1 Introduction

The 1974 Lithospheric Seismic Profile in Britain (LISPB) had the general aim of establishing a reliable cross-section of the lithosphere through the British Isles from the north of Scotland to the Channel. The *crustal* profiles were intended to:

(i) establish a detailed crustal velocity cross-section that would be useful to discussions of tectonic problems in the British Isles, in particular the evolution of the Caledonian orogenic belts,
(ii) provide essential control for the *long-range* profiles which were intended for the study of structure in the lower lithosphere (e.g. Faber & Fuchs 1977).

* Present address: Geophysikalisches Institut, Universität, Karlsruhe, Germany.
† Geophysics Section, School of Cosmic Physics, Dublin Institute of Advanced Studies, Eire.

This paper presents LISPB results for the *P* velocity structure of the crust and uppermost mantle beneath Northern Britain.

2 The LISPB experiment: data and travel-time correlations

The LISPB experiment has been fully described in Bamford *et al.* (1976) and Kaminski *et al.* (1976); that part of the experiment relevant to studies of the crust and uppermost mantle beneath Northern Britain in shown in Fig. 1(a).

In brief, during 1974 July and August, 60 German and British seismic stations (recording three components of ground motion on magnetic tape) occupied at different times the three segments ALPHA, BETA and GAMMA. Shots were fired at the various shotpoints to build up a series of reversed and overlapping crustal profiles (Fig. 1(b)) with observations out to at least 180 km distance, that is, sufficient for penetration to the Moho. In addition, a local earthquake (at KEQ – Fig. 1(a)) was well recorded whilst the stations were occupying segments ALPHA and BETA and a single test profile had been completed in 1973 August using land shotpoint 2 and recording slightly to the east of GAMMA (Fig. 1(a)).

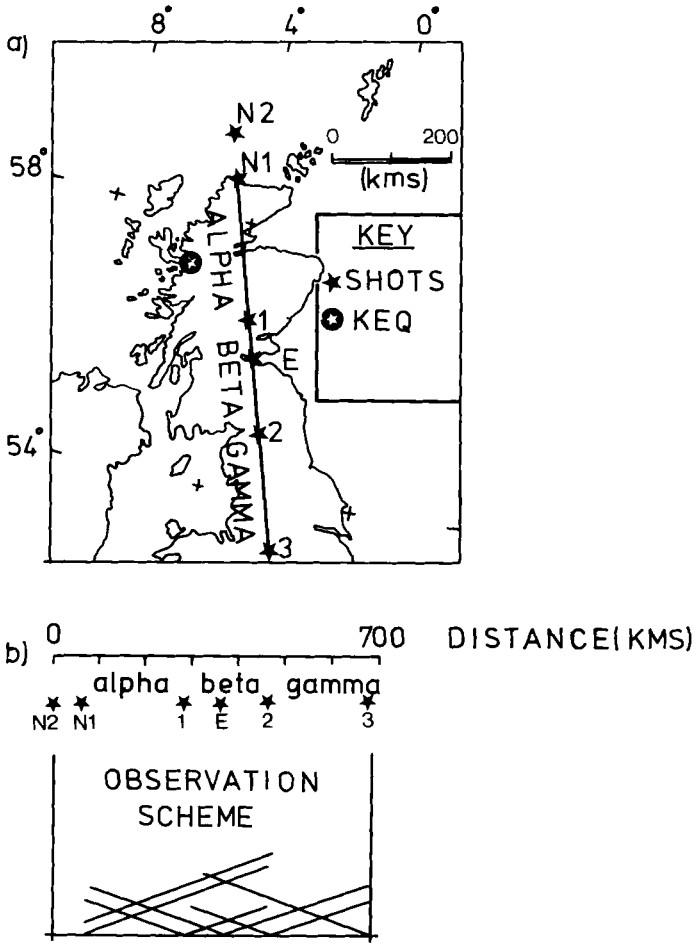

Figure 1. (a) Location of LISPB shots and profiles, Northern Britain. (b) Observation scheme for crustal profiles.

After the experiment, all the seismograms were digitized, scaled and filtered and then plotted in the form of time–distance record sections (Fig. 2).

The main aim in high-resolution seismic studies is to recognize or correlate in the record sections the various refracted and reflected arrivals returned from the seismic boundaries within the crust and upper mantle. Correlation is a relatively simple process for strong first-arrival refractions such as may be returned from the upper crust but it may be at best a subjective process when assessing weak, especially later, arrivals in the face of the time delays and other variations introduced by their passage through a highly heterogeneous crust. To aid the correlation process, geological and topographic sections were mounted beneath the record sections on the same horizontal scale and sections were plotted in a variety of ways: true amplitude record sections (as opposed to the normalized sections of Fig. 2) proved very useful whereas those with polarization filtering did not. Correlations were then based first of all on a semi-quantitative assessment of the effects of topography and near-surface geology upon the travel times, and later on a re-plotting of all the record sections with time corrections applied to each seismogram to take account of topography and near-surface geology.

Bearing in mind the variations in geologic/tectonic structure crossed by the profile, it would be unlikely that a single system of travel-time curves could be recognized which, with only small fluctuations, would apply to all observations and indeed the correlations made (described with a simple alphabetic notation and shown in Fig. 2) do imply considerable lateral inhomogeneity in the crust of Northern Britain. Nevertheless, the following generalizations – based on the summary travel-time curves of Fig. 3 – are possible.

The a curves are first-arrival refractions on seismograms at observation distances up to 120 or occasionally, 150 km.

The phase a_s is a refracted (or direct) arrival through the uppermost layers, usually the sediments and a_0 is a refracted arrival through the uppermost basement. Thus in the Midland Valley of Scotland, for example, the a_s velocities of 4–5 km/s observed from shotpoint E (Figs 2(e) and (f)) relate to the Old Red Sandstone/Lower Carboniferous sequence whereas the a_0 velocities of slightly less than 6 km/s define Lower Palaeozoic rocks.

The phase a_1 behaves somewhat irregularly though it is clearly of higher velocity than a_0 (say, greater than 6.2 km/s) and is refracted from a deeper interface.

At greater observation distances, the a phases are replaced by a first-arrival, phase d, with apparent velocity in the range 7.9–8.3 km/s. This is the Moho refraction (conventionally

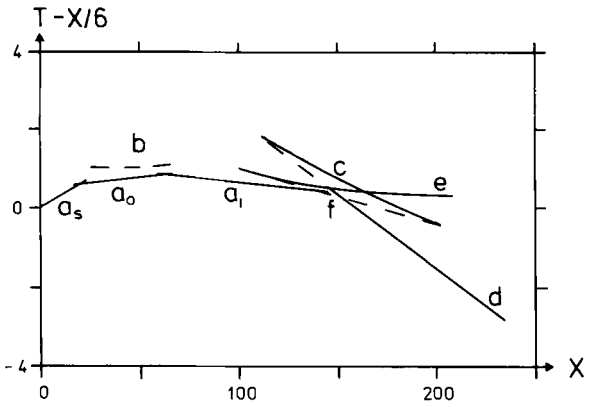

Figure 3. Summary of travel-time curves, reduced travel time ($T-X/6$ s) versus distance (X, km). Solid lines indicate arrivals seen on several sections, broken lines those seen on only a few sections.

termed P_n); it should be noted that d eventually dies away at a distance of somewhat less than 300 km (the exact value depends on the size of shot) to be replaced by much stronger and slightly faster phases which have clearly penetrated the lower lithosphere and are observed from distances of 200–250 km onwards. The profile N2 $-\alpha+\beta$ (Fig. 2(a)) shows this effect quite clearly, as does E $-\beta+\alpha$ (Fig. 2(e)).

The phase c, tangential to d at shorter ranges, is the Moho reflection (conventionally termed P_MP).

Phase e is often a very strong phase, for example on profiles N2 $-\alpha+\beta$ and N1 $-\alpha+\beta$ (Figs 2(a) and (b)). Although it arrives close in time to the Moho reflection c at shorter distances and might appear to be its continuation, it is not in fact a simple reflection from the crust–mantle transition but seems to be related to structure in the lower crust. Its associated refraction f is only occasionally observed (e.g. Fig. 2(g)) and then with considerable uncertainty.

The designation b is reserved for weak arrivals of little horizontal persistence observed between the a and the e or c travel-time curves on one or two record sections (but not shown in Fig. 2). The variability of these arrivals and their position on the sections, indicates that they are most probably caused by energy reflected from mid-crustal velocity discontinuities which have little horizontal continuity and hence, significance.

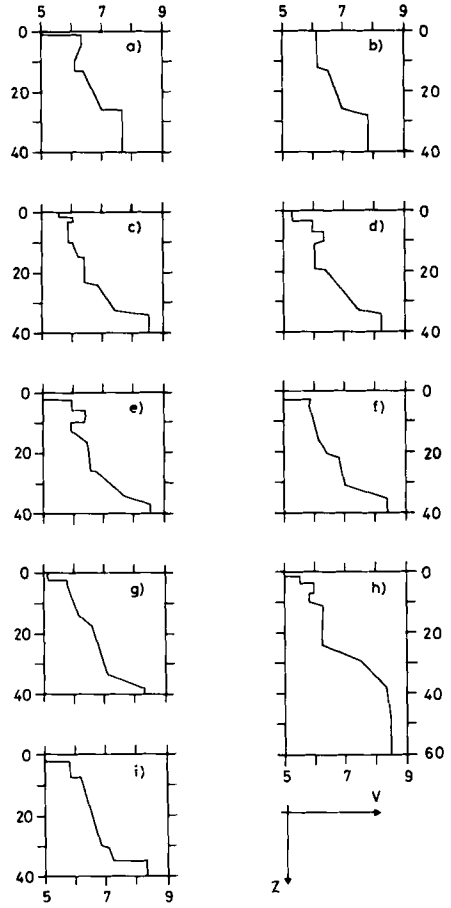

Figure 4. Velocity (V, km/s) versus depth (Z, km) functions for the record section: (a) N2 $-\alpha+\beta$. (b) N1 $-\alpha+\beta$. (c) 1 $-\alpha$. (d) 1 $-\beta$. (e) E $-\beta+\alpha$. (f) E $-\beta+\gamma$. (g) 2 $-\beta$. (h) 2 $+\gamma$. (i) 3 $-\gamma+\beta$.

As a preliminary step in interpretation, velocity–depth functions have been fitted to the travel-time curves for each section. These functions (Fig. 4) are based on assumptions of plane horizontal layering and give only a first-order indication of the crustal structure and its variation. Nevertheless, they do tend to confirm the suggestion contained in the correlations of Fig. 2 and especially in the variation in the e and c phases, of considerable variation in the structure of the lower crust and the crust–mantle transition. Note, for example, the relative difficulty in correlating phases e and c beneath GAMMA on profiles $2-\gamma$ and $3-\gamma+\beta$ (Figs 2(h) and (i)) as compared with N2 $-\alpha+\beta$ and N1 $-\alpha+\beta$ (Figs 2(a) and (b)) and the differences between the corresponding velocity–depth functions (Figs 4(h) and (i), (a) and (b) respectively).

It should be emphasized that the correlations shown in Fig. 2 are primarily descriptive. Individual travel times have been read from the record sections for each phase and the resulting time–distance data forms the basis for detailed interpretation. All interpretation is based on data corrected for the effects of topography.

3 The upper crust (the a phases)

The interpretation of first-arrival refraction time–distance data is straightforward (see also Bamford *et al.* 1977). The approach adopted has been to use various inverse techniques such as plane dipping-layer solutions and the plus–minus method (Hagedoorn 1959) to establish refractor velocities and a first estimate of depths to interfaces beneath different parts of the profile. It should be noted that, in addition to the LISPB observations, data from one other seismic experiment are crucial to this initial assessment of velocities and depths. The 1972 North Atlantic Seismic Project (NASP, Smith & Bott 1975) gave the following results for the North Scottish Shelf region (roughly north and east of LISPB segment ALPHA – Fig. 1(a)).

P_g, velocity 6.10 ± 0.15 km/s, close to the surface,
P^*, velocity 6.48 ± 0.06 km/s, varying in depth from 2 to 16 km beneath the Caledonian foreland and also identified beneath the western part of the Caledonian fold belt and the Moray Firth.

From the distribution and apparent velocities of the travel-time branches, the LISPB phases a_0 and a_1 are identical to Smith & Bott's P_g and P^* respectively.

A computer-based ray-tracing method (Cerveny, Langer & Psenčik 1974) – suitable for laterally inhomogeneous media – was then used to study the propagation, especially the

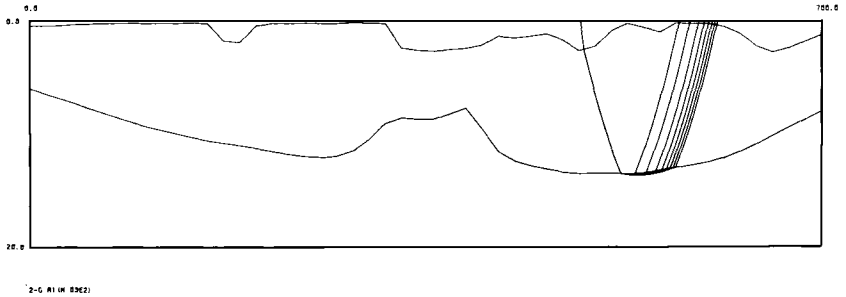

Figure 5. Simple example of ray-tracing through a laterally inhomogeneous medium. This model represents an early stage in the modelling of the upper crust with the velocities as in Fig. 6 but the final positions for the interfaces not yet determined.

travel times, of particular rays through the complete model (e.g. Fig. 5). By iterative adjustment of the model, observed travel times have been fitted, after correction for topography, to 0.1 s or better. The main features of the resulting upper crustal model are shown in Fig. 6.

The velocities for the uppermost layers are based either on observed a_s velocities where available or on documented velocities.

3.1 LAYER a_0

On segment ALPHA, the true velocity for a_0 must be close to the apparent velocities as the arrivals appear to be either a refraction from very shallow depth or a direct wave. The 6.0–6.2 km/s values (Fig. 6) correspond well with the 6.10 ± 0.15 km/s NASP value.

On BETA and GAMMA however, a_0 is clearly characterized by a lower velocity of 5.7–6.0 km/s. Plus–minus analyses for shotpoints 1 and E give a velocity of 5.93 ± 0.03 km/s beneath the Midland Valley, and for shotpoints E and 2 a velocity of 5.84 ± 0.02 km/s beneath the Southern Uplands. In ray-tracing, the a_0 phase can best be fitted if a slight increase in velocity with depth is permitted within the layer, especially beneath segment BETA (Fig. 6).

Generally the depths to the top of this uppermost basement simply show the sedimentary thickness, although occasionally the low-velocity superficial layer is probably related to a zone of fractured and unconsolidated basement rock, for example in the Southern Uplands (Fig. 6).

Clearly the changes in the velocity of this layer, shown in Fig. 6 as taking place at Loch Tay and the Great Glen, are important features. There is one other point of interest. There is a considerable difference between the horizontal distance over which a_0 is observed on profiles which cross the Midland Valley (20–50 km on profiles $1-\beta$ and $E-\beta+\alpha$, Figs 2(d) and (e)) and that for profiles which cross the Southern Uplands (20–120 km on profiles $E-\beta+\gamma$ and $2-\beta$, Figs 2(f) and (g)). To model these differences with the relatively weak velocity gradients implied by the almost linear a_0 travel-time branches, it is necessary for the a_0 (i.e. Lower Palaeozoic) sequence to be much thicker under the Southern Uplands than the Midland Valley (Fig. 6).

3.2 LAYER a_1

The main feature of the a_1 travel-time branch is its variability. In particular, it becomes a well defined first-arrival by 80–100 km observation distance in the far north of Scotland, at 50 km distance in the Midland Valley and again at 80–90 km distance in northern England. However, on profile $1-\alpha$ (Fig. 2(c)), between the Great Glen and Loch Tay Faults, the phase a_1 may be totally absent. Beneath the Southern Uplands, the phase a_0 is not replaced as a first-arrival until beyond 120 km distance and then not by a_1 but by deeper penetrating phases (Figs 2(f) and (g)). Furthermore, the clear a_1 arrivals of 6.4–6.5 km/s apparent velocity observed at distances over 50 km on profiles $1-\beta$ and $E-\beta+\alpha$ (Figs 2(d) and (e)) degenerate into weaker, slower arrivals, designated a_1': this behaviour (and the absence of a definite a_1 on $1-\alpha$) might result from the fairly rapid deepening (e.g. due to a major down-faulting) of the interface propagating the a_1 refraction.

Beneath the segment ALPHA and the Midland Valley the a_1 arrivals seem to be related to a velocity similar to the 6.48 ± 0.06 km/s NASP estimate, indicating that this layer most probably extends from the shelf into the Midland Valley. The lack of reversed coverage suitable for a plus–minus analysis means that this can only be confirmed using plane-dipping layer models; apparent velocities of 6.4 km/s are observed on $N2-\alpha+\beta$, 6.8 km/s

on N1 $-\alpha+\beta$, 6.5 km/s on E $-\beta+\alpha$, 6.4 km/s on $1-\beta$ and 6.4 km/s on the KEQ $-\alpha+\beta$ section (Kaminski *et al.* 1976) – the mean of these values is 6.50 ± 0.17 km/s. For ray-tracing, this layer is found to be best represented (Fig. 6) by an increase in velocity with depth from 6.4 to a maximum of 6.45 km/s, the mean of which is within the error limits of both the mean apparent velocity and the NASP estimate.

Jacob (1969) has interpreted phase velocities observed at the EKA array as indicating that there is an approximately horizontal layer of 6.4 ± 0.10 km/s below the array in the Southern Uplands but the depth of 12 km was not closely controlled. The results indicated that the 6.44 km/s layer shoaled to the NE and SW. This is off the axis of LISPB and would not influence the present results. His results for the a_0 layer are similar and indicate, like LISPB, a velocity increase with depth.

Beneath GAMMA, a plus–minus analysis is possible for the a_1 arrivals and yields a velocity of 6.28 ± 0.04 km/s; after ray-tracing, an increase of velocity with depth from 6.25 to a maximum of 6.3 km/s is included in the model (Fig. 6).

The structure of the a_1 interface requires some elaboration, especially for the region between the Great Glen Fault and the Loch Tay Fault and for the Southern Uplands.

The continuation of the 6.4 km/s layer beneath the Great Glen–Loch Tay region is based upon the observation of this velocity within this region on the earthquake section KEQ $-\alpha+\beta$ (Fig. 6). However, the travel times of these arrivals cannot be used to fix the depth of this layer as the focal depth of the earthquake is itself only poorly known and the earthquake may in fact be within the 6.4 km/s layer (Kaminski *et al.* 1976). The only information that might constrain the depth in this region comes from the rather weak arrival a_1? on the profile $1-\alpha$ (Fig. 2(c)). Whilst the very low apparent velocity (6.1 km/s) of these arrivals together with their poor quality count against them being a genuine a_1 refraction, they are certainly the earliest arrivals on $1-\alpha$ that *could* be a_1 and hence the depth fitted to them by ray-tracing (Fig. 6) should represent a *minimum* depth.

Beneath the Southern Uplands, the problem is rather different. The ray-tracing program will only generate a refraction from an a_1 interface that is continuous between the Midland Valley and the Alston Block (Fig. 6) if this interface is placed at depths which predict a_1 first-arrivals at 90 km distance or less, that is at depths similar to, or only slightly greater than, those beneath GAMMA. This tends to confirm that those arrivals which do eventually replace the a_0 phase as a first-arrival but at distances beyond 120 km are correctly identified as deeper penetrating (lower crustal) phases.

There are no reflected phases on either E $-\beta+\gamma$ or $2-\beta$ (Figs 2(f) and (g)) which might yield a direct estimate of the thickness of the a_0 layer beneath the Southern Uplands and hence the question mark in Fig. 6 represents the only reasonable conclusion at this stage of modelling, although the thicknesses must be at least those shown.

4 The lower crust and uppermost mantle (phases e, c and d)

The phase d is the best observed of the LISPB phases in the sense that it is usually fairly clear, especially north of the Midland Valley and is observed on both reversed and overlapping profiles. Plus–minus analyses, dipping-layer solutions, etc. have been attempted but the most useful results have been obtained by time-term analysis, in particular by using the MOZAIC method of Bamford (1976) which allows the use of observation schemes that were not designed with time-term analysis in mind (as LISPB was not). Three time-term solutions are of interest here. The first, using only observations to the north of shotpoint E (in the Midland Valley), yielded a uniform velocity of 7.90 ± 0.05 km/s. The second, using a rather poorly distributed data set with only those observations south of shotpoint E, gave

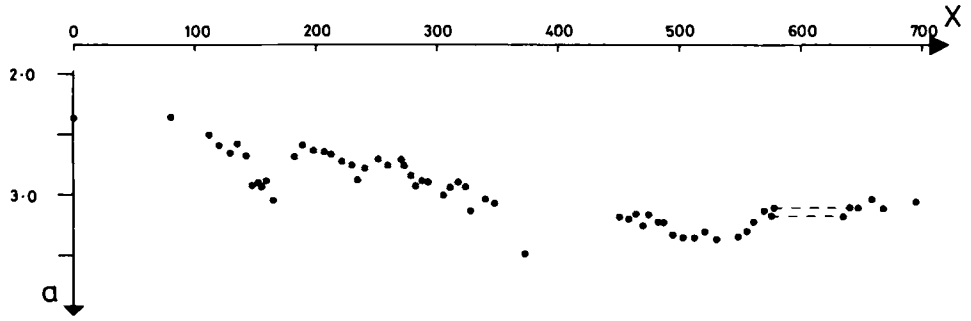

Figure 7. Phase d delay times (a, s) plotted as a function of distance (X, km) from N2.

a velocity of 8.03 ± 0.15 km/s. Finally, a combination of all available observations gave a uniform velocity of 7.99 ± 0.05 km/s; this compares well with the NASP estimate of 7.99 ± 0.02 km/s.

The delay-time profile resulting from these solutions is shown in Fig. 7; very approximately the delay times can be multiplied by 10 (± 1) to convert them to depths. In addition to the general increase in delay times (crustal thickening) as the profile approaches the Midland Valley, an intriguing aspect is the 'delay-time discontinuity' which seems to occur at around 160–170 km horizontal distance, apparently rather close to the surface position of the Great Glen Fault. However, in assessing the nature and significance of this horizontal discontinuity, it should be remembered that the point of critical refraction at the interface will, in studies of the continental Moho, be offset by some 30–40 km from the surface observation point. This means that any computed depth must be plotted with due allowance for such offsets and that, in time-term analysis where several observations at a surface site yield a single delay time at that site, that delay time in fact represents an average over the cone of critically refracted rays, a cone whose base will be 60–80 km. Thus, as O'Brien (1968) has pointed out, the time-term method may produce biased results in the presence of a horizontal discontinuity and will be much less effective in studying such a discontinuity than other techniques which take more account of the paths actually travelled by the rays. Ray-tracing in fact indicates that the horizontal discontinuity should be displaced by about 30–40 km to shorter horizontal distances.

For the interpretation of the wide-angle reflections e and c, the technique devised by Bamford (1978) has been used. First the effects of refraction in the layers above the reflector are removed by correcting, using ray-tracing, to a datum in the layer immediately above the reflector. The corrected time–distance data may then be analysed in T^2–X^2 space, the exact method of analysis depending on the degree of subsurface coverage available. For example, if multiple common reflection-point coverage is available, a least-squares analysis will yield both the velocity immediately above the reflector and a depth below datum for every common reflection point. This approach is iterative and requires accurate information concerning the properties of the layers above the reflector of interest and an initial, reasonably reliable, approximation to the topography of the reflector and the velocity immediately above it. For phases e and c, the upper crustal structure already determined (Fig. 6) was used together with a combination of depths and velocities from the velocity–depth functions (Fig. 4) and the phase d time-term solutions. The smoothed and extrapolated starting model for the interpretation of phases e and c is shown in Fig. 8. Particular items of uncertainty in this model are the lower crustal velocities, shown in Fig. 8

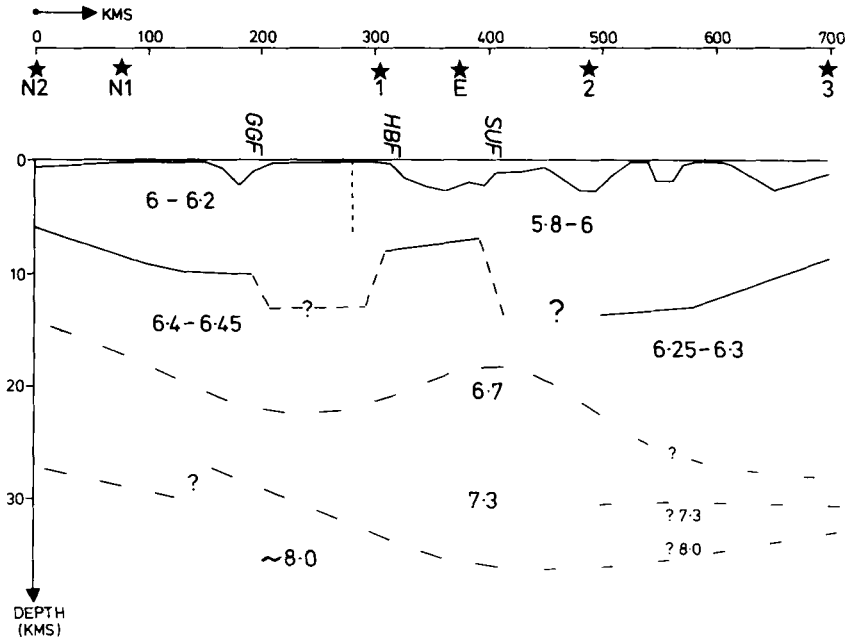

Figure 8. Preliminary model used as a basis for the interpretation of phases e and c.

as 6.7 to 7.3 km/s, and the configuration of the lower crust and the crust–mantle transition beneath the southern half of BETA and beneath GAMMA.

Unfortunately neither phase e nor c were observed with any significant amount of multiple coverage (Figs 9 and 10) and so in neither case could the independent determination of the velocity above the reflector *and* the reflector topography be attempted. The approach used therefore, was to assume that the velocity above the reflector was broadly correct and to calculate using this velocity a depth below datum for each reflection point from the datum-corrected T^2–X^2 data; then in addition to adjusting reflector topography

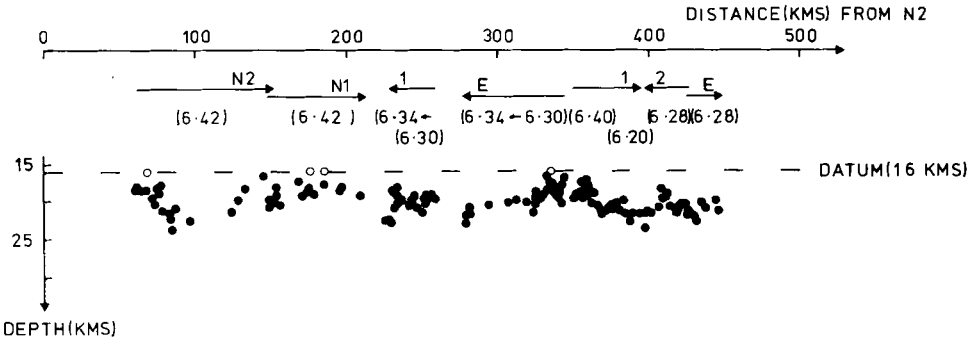

Figure 9. Depths computed for phase e. $\xrightarrow[(6.42)]{\text{N2}}$ Subsurface coverage from a given shotpoint and rms velocity above reflector. • Depth value. Occasionally a zero (or even negative) datum-corrected travel time may result. A zero (or negative) depth may then be computed: for convenience, all such values are shown (○) as lying at the datum depth.

during iteration, such minor adjustments in velocity were made as were necessary to produce where possible, a continuous reflector.

Generally, this approach worked well beneath segments ALPHA and BETA but various problems were encountered beneath GAMMA.

4.1 ALPHA AND BETA

For phase e, the iterative process proved particularly slow, primarily because of the relatively complicated velocity structure above the reflector but, after seven iterations, the depths shown in Fig. 9 stabilize in a model in which the average velocities above the reflector are little different from those of Figs 6 and 8. However, some additional information has been obtained about the two regions of uncertainty in the a_1 layer of Figs 6 and 8.

In Fig. 9, an average velocity of less than 6.4 km/s is required between the Great Glen and Loch Tay Faults if the a_1 interface is kept at the depth shown in Figs 6 and 8: this confirms that this is in fact a *minimum* depth to this interface.

Beneath the Southern Uplands, consistent depth values can be obtained in the horizontal distance range 400 to 450 km (for profiles $E-\beta+\gamma$ and $2-\beta$ which observe in opposite directions) by extending the 6.25–6.3 km/s a_1 velocities further north than is shown in Figs 6 and 8. On the other hand, e reflections on profile $1-\beta$ that bottom beneath the Midland Valley are indicative of an average velocity of 6.4 km/s whilst those which bottom beneath or close to the surface position of the Southern Uplands Fault require average velocities closer to 6.2 km/s. This interesting effect cannot be uniquely modelled because of insufficient data but, as in the upper crustal modelling, such evidence that there is suggests that the a_1 layer may not be continuous across the Southern Uplands and that it is possible that the horizontal discontinuity occurs at or immediately south of the Southern Uplands Fault.

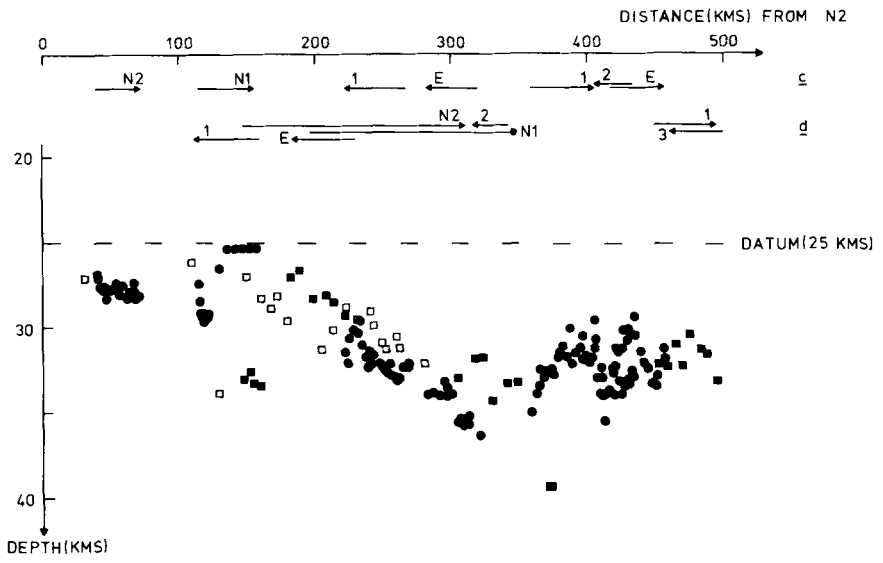

Figure 10. Depths computed for phases c and d. $\xrightarrow{N2}$ Subsurface coverage for a given shotpoint. • Depth value, phase c. • Depth value, phase d. □ Depth value, phase d, from observations in a single direction only and so plotted offset by 30 km in the direction of observation.

The scatter of the depth values in Fig. 9 precludes any attempt to recognize other than the broad details of the topography of the e reflector.

Data relating to phase c is even less well distributed than that for e and correspondingly less information can be extracted from it. However, early attempts at ray-tracing indicated that consistent results could *not* be obtained if the gradient in velocity from 6.7 to 7.3 km/s was retained in the layer above the reflector (Fig. 8) – a layer of uniform velocity 7 km/s was found to be the most effective. No further adjustments in velocity were necessary to produce, after two iterations, the depths shown in Fig. 10. Provided those depths derived for d delay times based on observations in a single direction (e.g. between 225 and 310 km horizontal distance – Fig. 10) are corrected for the effect of offset, there is reasonable agreement between the depths computed for phases c and d. The depth profile retains the suggestion of a possible horizontal discontinuity close to 150 km horizontal distance though in view of the previously mentioned biasing of delay times close to horizontal discontinuities and the scatter of the depth values, it is difficult to say more than this.

4.2 GAMMA

For segment GAMMA, both the observation coverage (Fig. 1(b)) and the quality of the correlations for phases e and c that can be made on the record sections (Figs 2(h) and (i)) are much less satisfactory than for ALPHA and BETA. These two factors combine to make two-dimensional modelling of the lower crust beneath GAMMA a largely futile exercise.

The arrivals marked e on profile $2-\gamma$ (Fig. 2(h)) can be successfully modelled with a reflector at a depth of approximately 22–23 km forming the base of the 6.25–6.3 km/s layer (Figs 6 and 8) at about 550 km horizontal distance. Furthermore, modelling of phase c suggests that it may be associated with a reflector at between 25 and 30 km depth with an average velocity as high as 7.5 km/s *above* it. The phase d delay times beneath GAMMA, Fig. 7, then suggest Moho depths of 30–35 km.

The tentative and uncertain nature of this evidence cannot be over-emphasized but it does imply that the transition from lower crustal velocities (< 7.3 km/s) to typical upper mantle velocities (~ 8 km/s) may take place gradually over a depth range of more than 5 km, somewhat as suggested in Fig. 8 though not necessarily at those depths or velocities. If so, then the structure of the lower crust beneath GAMMA is rather different from that beneath ALPHA and BETA where the crust–mantle transition was modelled with a first-order discontinuity.

5 Regional Moho delay times and velocity anisotropy

A particularly interesting consequence of the LISPB type high-resolution seismic experiment is the opportunity it provides for a re-assessment or re-interpretation of data from previous experiments. For example a relatively high proportion of previous experiments around the British Isles have concentrated upon studying the Moho discontinuity using phase d, the Moho refraction (P_n), and this without being aware that this phase is in fact observable over only a limited distance range as found in LISPB (Figs 2 and 3) and earlier studies (Hirn *et al.* 1973; Bamford 1977).

In Northern Britain, data is available from several experiments in addition to LISPB; these include NASP (Smith & Bott 1975), the Norway–Scotland P_n Project (Sornes 1968), the ten-ton shot program (Jacob & Willmore 1975) and the various explosions fired around Scotland known collectively as the Scottish Offshore Seismic Programme (SOSP, Jacob 1975). Recordings are available from both mobile stations and the LOWNET array (Crampin

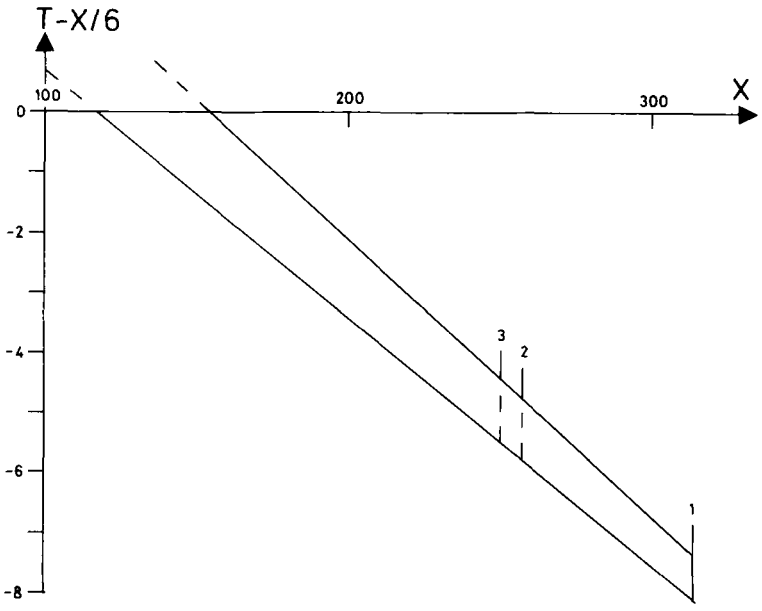

Figure 11. LISPB phase d envelope, reduced time versus distance. Maximum observation distances: (1) LISPB; (2) NASP; (3) SOSP, Norway–Scotland P_n, ten-ton shots.

et al. 1971) in central Scotland. The available data, in some cases like NASP consisting of time–distance values (Smith 1975, unpublished PhD thesis) or, for all shots recorded on LOWNET, replayed and re-picked seismograms, have been assessed using the LISPB based time–distance envelope of Fig. 11. An arrival was accepted as phase d only if its time–distance value lay inside this envelope; due allowances were made for the variations in shot sizes between the different experiments. Whilst the quality of the observations was sometimes well below that of LISPB, in particular for the SOSP shots as recorded on LOWNET, over 430 travel times, weighted according to their quality relative to LISPB, were acceptable as phase d. These observations were derived from the shots and stations shown in Fig. 12.

In addition to the study of regional Moho delay times, this data also offers the opportunity to study possible velocity anisotropy in the uppermost mantle. The main condition for the study of such anisotropy is that there should be a relatively even distribution of observations as a function of azimuth through essentially the same subsurface. Whilst the geographic distribution of shots and stations (Fig. 12) and the azimuthal distribution of observations (Fig. 13) are far from ideal, they are, coupled with the careful selection of data, considered to offer a real possibility for the study of anisotropy using the MOZAIC method (Bamford 1976, 1977) though anisotropy functions resulting from the study might well be suspect in detail.

However, velocity anisotropy seems most definitely *not* to be required by the data. For example, the complete data set gave a variance of 0.035 s^2 if a uniform refractor velocity was assumed as compared with 0.034 s^2 if velocity anisotropy was allowed. On the other hand, omission of the relatively uncertain SOSP data, gave a variance of 0.027 s^2 for a uniform velocity solution, 0.028 s^2 for an anisotropic solution. Several other data combinations were attempted but the only justifiable conclusion was that a uniform velocity of 7.97 ± 0.03 and the delay times of Fig. 14 were the best results obtainable.

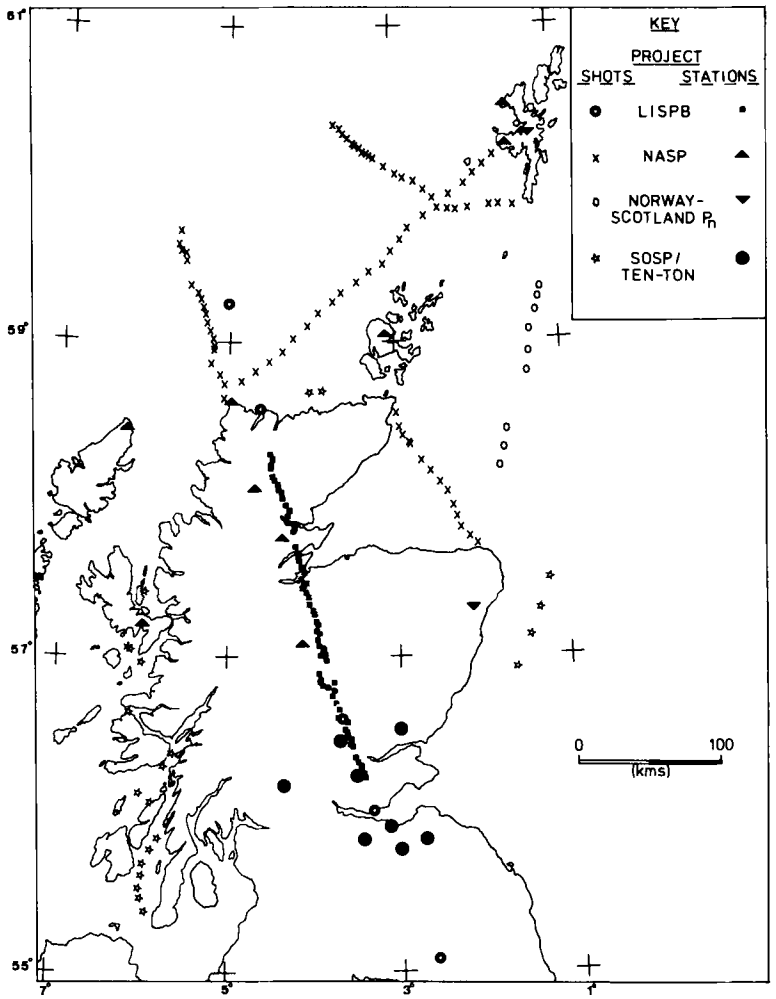

Figure 12. Distribution of shots and stations contributing phase d time–distance data, Northern Britain. The LOWNET stations are those identified as recording SOSP shots.

6 Discussion

The objective modelling processes used in the foregoing interpretations are built on a subjective base, the correlations on the record sections (Fig. 2). In truth, once the correlations have been made, many aspects of the final model are fixed. In the simplest example, that of a single profile interpreted in terms of a plane horizontally layered model, the correlations define exactly the velocities, and ultimately the layer thicknesses, except in cases of ambiguity such as low-velocity zones. Thus, the velocity–depth functions of Fig. 4 can be regarded as simply a quantitative description of the correlations in Fig. 2. Clearly the relationship between the correlations and a laterally inhomogeneous model is more complicated but, as an example, the Moho 'step' found at about 150 km distance (Figs 7, 8 and 10) was inevitable, at least in some form, once the phase d correlation on N2 $-\alpha+\beta$ and the phase c correlation of N1 $-\alpha+\beta$ (Figs 2(a) and (b)) had been drawn with the breaks in the curves as shown. In addition, different workers will usually differ about the details of

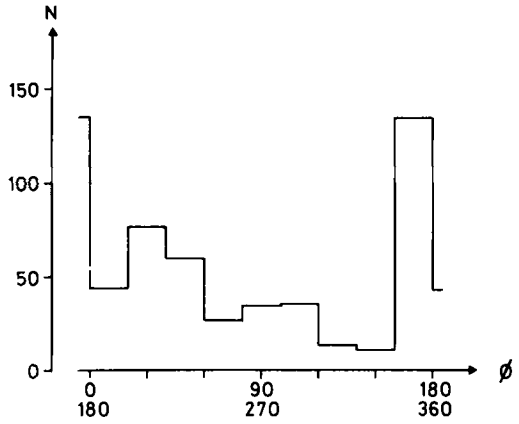

Figure 13. Histogram of number (N) of phase d observations versus azimuth (ϕ, degrees E of N).

correlations and the picking of arrival times and sometimes will differ about the number, or nature, of travel-time curves required on a particular record section.

Furthermore, any refraction or wide-angle reflection observation scheme tends to average horizontally the actual structure, sometimes over tens of kilometres and thus even with the relatively close station spacing available in LISPB, fine details of any model may be highly suspect.

Thus it is assumed that only the broad elements of the computed models are reliable and probably repeatable if the LISPB data were to be independently interpreted. The resulting cross-section is shown in Fig. 15, and has the following features:

(i) A superficient layer which includes Upper Palaeozoic and more recent sediments.

(ii) An upper crustal sequence with velocity dependent on the area: to the north this layer (6.1–6.2 km/s) may be interpreted as Caledonian belt metamorphics. South of Loch Tay velocities of 5.8–6.0 km/s define the Lower Palaeozoic sequence.

(iii) The layer with a velocity of 6.48 ± 0.06 km recognized by Smith & Bott (1975) and identified by them as granulite facies Lewisian basement rocks probably extends from the Caledonian foreland into the Midland Valley but appears to terminate at the Southern Uplands Fault. The depth of this layer varies between 6 and 14 km.

To the south, a layer of lower velocity 6.28 ± 0.04 km/s, underlies the Lower Palaeozoic sequence at a depth of 8–14 km. This value is significantly different from the NASP value of 6.48 ± 0.06 km/s but it is extremely doubtful whether the latter, derived from a different experiment in a somewhat different geographical area, truly summarizes the horizontal and vertical velocity variations that might occur through this layer due to small differences in metamorphic grade, microcracking, anisotropy and so on. The LISPB estimates of this layer's velocity are 6.50 ± 0.17 km/s, a poor estimate from five apparent velocities and a velocity constrained between 6.4 and 6.45 km/s by the modelling of the refractions and the deeper penetrating wide-angle reflections.

The LISPB experiment suggests, but no more than that, that there is a change in the velocity of this layer from north to south with the horizontal transition placed at, or just south of, the Southern Uplands Fault. Only a considerable number of separate measurements on this layer throughout Northern Britain could demonstrate whether this difference is significant.

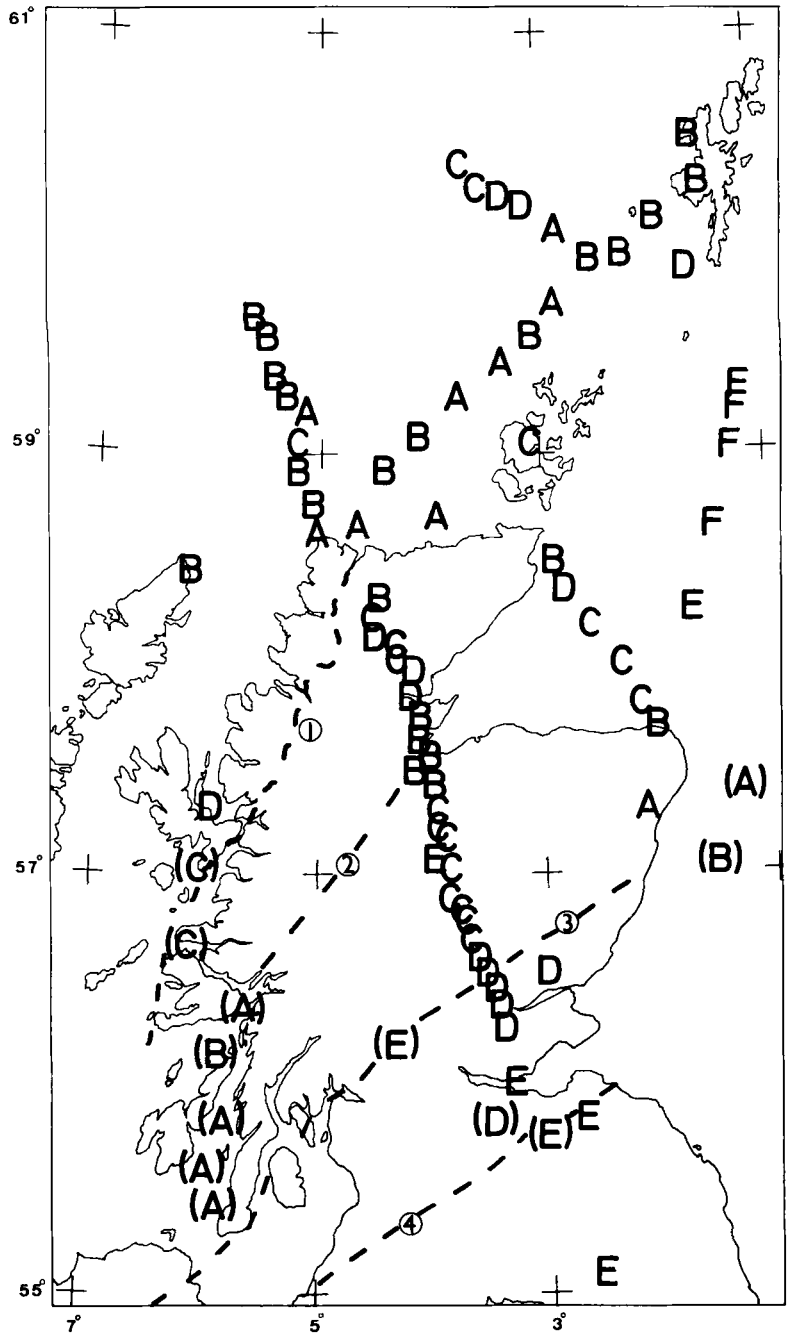

Figure 14. Delay time map, Northern Britain. To give a clearer picture in the face of the typical uncertainties of ± 0.1 s or more in computed delay times, the values have been graded according to the following scheme: A, < 2.4 s; B, 2.4 - 2.6; C, 2.6 - 2.8; D, 2.8 - 3.0; E, 3.0 - 3.2; F, > 3.2. The MOZAIC method usually assigns a single delay time to a small area rather than to one point (Bamford 1976); the graded values have been plotted at the mid-points of these areas. The values in brackets are those based entirely on SOSP data and may be relatively unreliable. Also identified on this map as thick broken lines are the surface expressions of: ① Moine Thrust; ② Great Glen Fault; ③ Highland Boundary Fault; ④ Southern Uplands Fault.

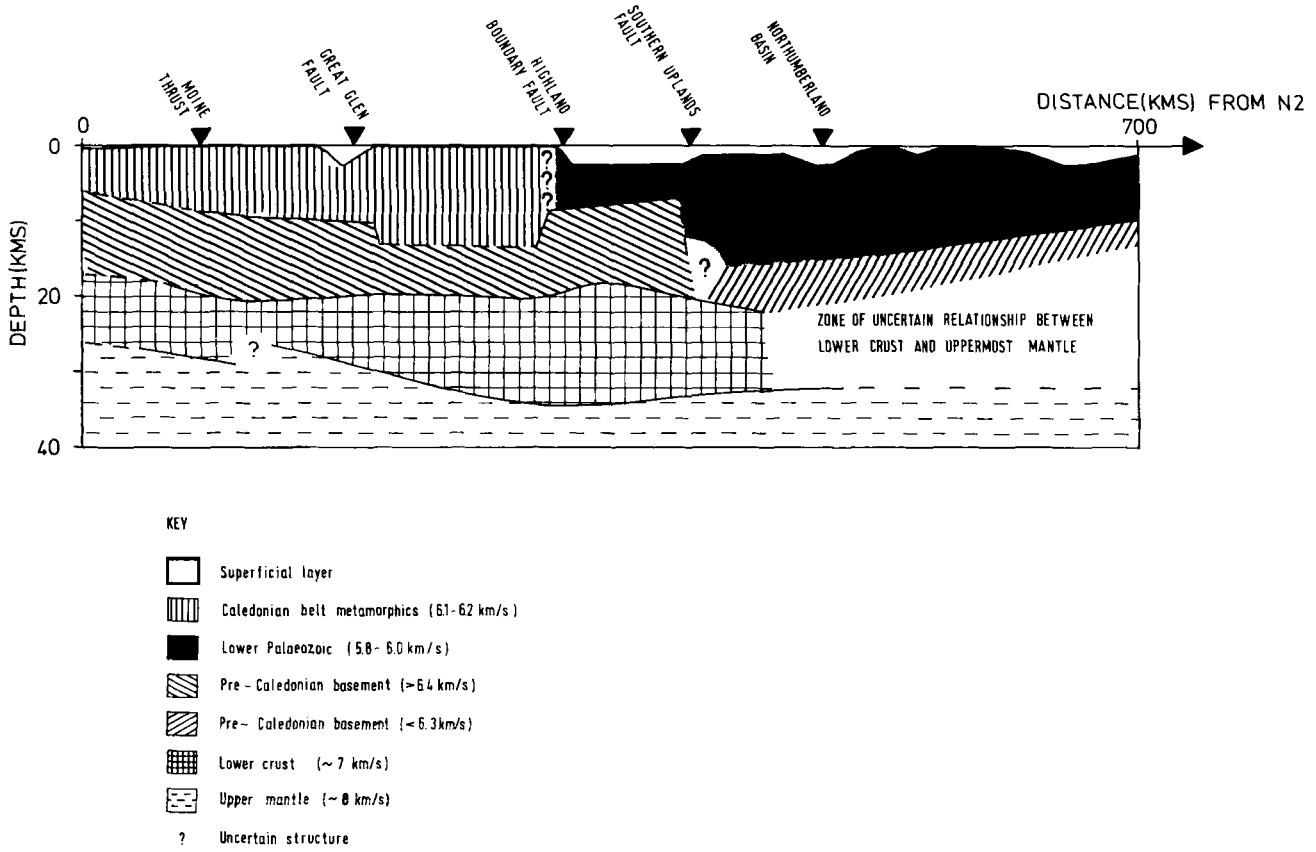

Figure 15. Schematic cross-section through the crust and uppermost mantle of Northern Britain.

This layer most probably defines the pre-Caledonian basement.

(iv) A lower crustal layer, with velocity approximately 7 km/s and at a depth close to 20 km, shallows slightly northwards and beneath the Midland Valley but may be either absent or simply poorly defined to the south.

(v) Both the LISPB and the regional analysis of sub-Moho velocity indicate that a uniform value close to 8 km/s is acceptable. No velocity anisotropy appears to be present and lateral variations are statistically insignificant.

The crust is relatively thin beneath the foreland region (low delay times – Fig. 14), thickening to the south beneath the Caledonian belt and the Midland Valley.

To the north the crust–mantle boundary can be defined by a sharp transition, a first-order discontinuity. Beneath GAMMA however, the form of the correlations, the velocity–depth functions (Figs 2 and 4) and such modelling as can be carried out given the lack of data, suggest a more gradual change from lower crustal to upper mantle velocities. The position of the change from one Moho type to another is especially uncertain.

Clearly, these results have considerable implications for the study of Caledonian tectonics, not least in their suggestion of differing crustal structures north and south of the Southern Uplands. In the hope that knowledge of Poisson's ratio variations would provide a further discriminant between crustal units and therefore permit more definite conclusions, a considerable effort has been also put into the study of LISPB shear waves and results are reported elsewhere (Assumpcao & Bamford 1978). The primary result of this study indicates that whereas Poisson's ratio throughout most of Northern Britain is close to 'normal' values of 0.25 (except for higher values in the sediments), anomalously low values are found in the a_1 layer just north of the Southern Uplands Fault and in the a_0 layer just south of it. Thus both the *P* and *S* data from the LISPB experiment give a strong indication of the primary significance of the Southern Uplands Fault in the tectonics of Northern Britain.

Acknowledgments

The LISPB experiments were supported by the Natural Environment Research Council and the Deutsche Forschungsgemeinschaft.

Digitization and plotting of the record sections were carried out at the Geophysikalisches Institut, Universität Karlsruhe. We especially acknowledge the help of our colleagues Werner Kaminski and Sonja Faber.

We are grateful to Professor M. H. P. Bott for his kind permission to make use of the NASP data.

References

Assumpcao, M. & Bamford, D., 1978. LISPB – V. Studies of crustal shear waves, *Geophys. J. R. astr. Soc.*, **54**, 61–73.

Bamford, D., 1976. MOZAIC time-term analysis, *Geophys. J. R. astr. Soc.*, **44**, 433–446.

Bamford, D., Faber, S., Jacob, B., Kaminski, W., Nunn, K., Prodehl, C., Fuchs, K., King, R. & Willmore, P., 1976. A lithospheric seismic profile in Britain – I. Preliminary results, *Geophys. J. R. astr. Soc.*, **44**, 145–160.

Bamford, D., 1977. P_n velocity anisotropy in a continental upper mantle, *Geophys. J. R. astr. Soc.*, **49**, 29–48.

Bamford, D., Nunn, K., Prodehl, C. & Jacob, B., 1977. LISPB – III. Upper crustal structure of Northern Britain, *J. geol. Soc. Lond.*, **133**, 481–488.

Bamford, D., 1978. Interpretation of wide-angle reflection travel-times in realistic crust–mantle structures, *J. Geophys.*, **45**, in press.

Cerveny, V., Langer, J. & Psenčik, I., 1974. Computation of geometric spreading of seismic body waves in laterally inhomogeneous media with curved interfaces, *Geophys. J. R. astr. Soc.*, **38**, 9–20.

Crampin, S., Jacob, B., Miller, A. & Neilson, G., 1971. The LOWNET radio-linked seismometer network in Scotland, *Geophys. J. R. astr. Soc.*, **21**, 207–216.

Faber, S. & Fuchs, K., 1977. *Struktur des oberen Erdmantels unter den britischen Inseln* (abstract), 37th Meeting German Geophys. Soc., Braunschweig 1977.

Hagedoorn, J. G., 1959. The plus–minus method of interpreting seismic refraction sections, *Geophys. Prospect.*, **7**, 158–182.

Hirn, A., Steinmetz, L., Kind, R. & Fuchs, K., 1973. Long-range profiles in western Europe – II. Fine structure of the lower lithosphere in France (southern Bretagne), *Z. Geophys.*, **39**, 363–384.

Jacob, B., 1969. Crustal phase velocities observed at the Eskdalemuir Seismic Array, *Geophys. J. R. astr. Soc.*, **18**, 189–197.

Jacob, B., 1975. The Scottish seismic refraction programme, pp. 325–328, *Proc. XIII Assem. European Seism. Comm.*, Brasov 1972.

Jacob, B. & Willmore, P., 1975. 10 ton explosions fired in 1971 and 1972, pp. 329–337, *Proc. XIII Assem. European Seism. Comm.*, Brasov 1972.

Kaminski, W., Bamford, D., Faber, S., Jacob, B., Nunn, K. & Prodehl, C., 1976. A lithospheric seismic profile in Britain – II. Preliminary report on the recording of a local earthquake, *J. Geophys.*, **42**, 103–110.

O'Brien, P. N. S., 1968. Lake Superior crustal structure – a reinterpretation of the 1963 seismic experiment, *J. geophys. Res.*, **73**, 2669–2689.

Smith, P. J. & Bott, M. H. P., 1975. Structure of the crust beneath the Caledonian Foreland and Caledonian Belt of the North Scottish Shelf Region, *Geophys. J. R. astr. Soc.*, **40**, 187–205.

Sornes, A., 1968. P_n time-term survey Norway–Scotland 1967, ARPA NO. 612–1, *Supp. Sci. Rep.*, 33 pages.